ISSN NO. 2320-5407

Journal homepage:http://www.journalijar.com

INTERNATIONAL JOURNAL OF ADVANCED RESEARCH

RESEARCH ARTICLE

Size dependent structural, electronic and vibrational properties of Cd_mS_n (m+n=2–6) nanoclusters: a DFT study

Rajkamal Shastri[1], Devesh Kumar[1], S.P.Goutam[1], R.R. Yadav[2] and Anil Kumar Yadav[1]*

1. Department of Applied Physics, Babasaheb Bhimrao Ambedkar University, Lucknow- 226025, U.P., India

2. Department of Physics, University of Allahabad, Allahabad- 211002, U.P., India

Manuscript Info

Manuscript History:

Received: 18 October 2015
Final Accepted: 26 November 2015
Published Online: December 2015

Key words:

Nanoclusters, Electronic, Vibrational, DFT, HOMO-LUMO, DOS, Binding energy, IP and EA

Corresponding Author

Dr. Anil Kumar Yadav

Abstract

We have performed first-principle calculations on the possible structures of cadmium sulphide Cd_mS_n (m+n=2–6) clusters; and equilibrium geometries, stabilities and electronic properties have been systematically investigated by density functional theory. Furthermore, binding energy (BE), highest-occupied and lowest-unoccupied molecular orbital (HOMO–LUMO) gap, density of states (DOS) have also been computed for Cd_mS_n nanoclusters. For the most stable structures, vibrational frequencies, infrared intensities (IR Int.), relative infrared intensities (Rel. IR Int.) and Raman scattering activities have been computed. The optimized geometries exhibit that the occurrence of the most stable configurations of the CdS nanoclusters is directly related to final binding energy. The nonlinear structured CdS_3 (rhombus) nanocluster with FBE 3.24 eV is found to be most stable as compared to others. We expect that findings of this study will stimulate further new experimental study on it.

INTRODUCTION

Nanoclusters represent the intermediate phase between small molecular species and the bulk state.The knowledge of atomic structure of nanoclusters is essential as their physical and chemical properties change significantly as size decreases from bulk level to nanoscale. Two basic reasons namely, quantum confinement effect and higher surface to volume ratio are viewed as vital for the dramatic change in their physical and chemical properties. To study the physical properties of such clusters it is indispensible to have an understanding about cluster evolution and possible structural changes that arise as a function of the nanocluster size because it can lead to the tailoring of novel materials with desirable properties [1]and sizes of the electronic devices have been reduced [2,3]. The basic idea behind structural study of the nanocluster is the assumption that it will follow structure with minimum energy. Therefore, global minimization techniques are used to predict the structure of nanoclusters. II–VI semiconductors such as ZnS, CdSe and CdTe are of enormous technological importance in different branches of science and technology. These semiconductors are widely used in solar cells, electronic sensors, hydrogen generation, photo catalysis and biological detections [4-9].Among the II–VI semiconductors, cadmium sulfide (CdS) is an important inorganic semiconductor owing to its unique photoelectric properties. It holds particle-size-dependent electronic spectrum [10,11] which could show the influence of size quantization effects. Its potential applications have been exhibited in many fields such as the nonlinear optics [12] the photo electro chemical cells and heterogeneous photo catalysis [13,14] etc.

There have been many experimental and theoretical studies using different computational approaches that are focused on the clusters of various compositions that have important and promising applications [3-8]. For binary clusters $(CdS)_n$, a number of theoretical studies have been performed to the search for the geometrical structure of the lowest total energy isomers [15-30]. It turns out from previous studies that the $(CdS)_n$ structures (n = 4–7)

obtained in different studies as the lowest energy states, are often not the same. Specifically, controversy is found in the structure of the lowest total energy state of $(CdS)_4$. Three different structures were obtained. First one cubic structure as predicted by Gurin et al. [21] second a ring non-planar structure [22] a state with the square geometry [23].

To the best of our knowledge, no detailed DFT calculations have been performed on CdS nanoclusters with unequal number of m and n considering the various properties. And hence, in this work, we have applied DFT computations to analyze the structural stabilities, electronic properties, adiabatic and vertical ionization potential (IP) and electron affinity (EA), HOMO-LUMO, DOS and vibrational behavior of Cd_mS_n(m+n=6) clusters as a function of the cluster size.

2. Computational Methodology

The theoretical methods used in the present study are based on first principle calculations within the density functional theory. Density functional theory (DFT) is one of the promising and efficient methods to investigate electronic, optical properties and structural stability of nanostructures. Structural optimization was carried out using the hybrid gradient-corrected functional (B3LYP) in conjunction with LANL2DZ basis set within density functional theory as framed in the Gaussian-09 suit [31]. For the most precise calculations, LANL2DZ basis set incorporating effective core potential (ECP) has been adopted as the basic basis set. Initially, a number of possible structures for each Cd_mS_n clusters are constructed and then each geometrical structure was fully optimized. Minimum energy for each structure is achieved by relaxing the atomic positions. We have used GaussSum 3.0 [32] for the evaluation of density of states (DOS) spectrum. For the visualization of molecular orbitals, chemcraft software was used [33]. In order to have stability of nanoclusters, binding energy per atom of the nanocluster is defined by the equation-

$$BE = [mE(Cd) + nE(S) – E (Cd_mS_n)]/(m+n)$$

Where, E(Cd), E(S), and E(Cd_mS_n) are the total energy of isolated atoms Cd, S and Cd_mS_n clusters, respectively, and m+n is the total number of Cd and S atoms. For a more accurate calculation of binding energy of the system, the zero point vibrational energy is subtracted from the earlier calculated BE value[34]. Therefore, we have also calculated the harmonic vibrational frequencies and the corresponding zero point energy (ZPE) for all optimized structures. The harmonic vibrational frequencies of each optimized structures were evaluated by analytical differentiation of gradients; eventually the stability of nanoclusters is considered on the basis of final binding energy (FBE) thus obtained. In all fully optimized structures, the convergence of the system energy is obtained up to 10^{-7} meV and the forces of 10^{-3} eV/A° on each atom are achieved. The excellent agreements between the calculated and experimental data imply the reliability of our computational approach employed in this work.

3. Results and Discussion:

3.1. Geometries and stabilities of Cd_mS_n clusters

The exact determination of equilibrium structures for the clusters under consideration is a fundamental requirement for the discussion of cluster's properties and the variation of the chemical bond with the size of cluster. There may be existent various possible structures for a given number of atoms which are rather close in energy. It is therefore significant to evaluate the sensitivity of a given property with respect to structural changes. In this section, we will present the equilibrium structures and stabilities of clusters of binary compound CdS. We carried out first principle calculations on the various Cd_mS_n (m+n = 2-6) clusters to obtain the stable isomers in each size range. The optimized most stable structures are presented in Fig. 1, while the symmetry, multiplicity of the ground state, HOMO−LUMO gap, binding energies and the final binding energy for all the optimized structures are listed in Table 1. The most stable isomers of Cd_mS_n clusters (m+n = 2-6) -linear, trigonal, rhombic, and star geometries, respectively, which are quite comparable to other reports, are shown in Table 2. The calculated bond lengths of Cd-Cd, Cd-S, and S-S for the most stable structures are appended in the Table 3. In the following, a discussion of the considered nanoclusters has been given.

CdS: Fig. 1(a) shows that the only possible structure for CdS cluster is linear molecule with final binding energy 2.38 eV and the Cd–S bond length 2.65A°. This equilibrium distance is much similar to the value 2.36 A° computed by Chu et al. [35] and experimental result 2.52 A° [36]. The multiplicity of ground state of this nanocluster is of triplet in nature.

Cd_mS_n (m + n = 3): For this cluster, three structures are possible which are the S-terminated linear structure, S-centered linear structure and trigonal structure. For Cd_2S configuration, ground states of the linear and triangular structures are of singlet and triplet in nature whereas for CdS_2 configuration, the predicted ground states for the linear and triangular structures are triplet.

For the **Cd_2S** configuration, It is clear from Table1 that the triangular structure with C_1 symmetry and the triplet ground state has maximum FBE (3.05 eV). The other two structures, linear Cd-Cd-S and Cd-S-Cd have lower FBEs in comparison to trigonal Cd_2S structure. Obtained Cd–S and Cd-Cd bond lengths for the trigonal structure are 2.59 A° and 4.06 A°, respectively as can be seen in Table 3. In the sulphur excess triatomic CdS_2, a similar structure to that of the Cd_2S are predicted. Among these, trigonal structure of CdS_2 with C_S symmetry has FBE of 2.22eV and is found to be most stable. The other two structures, linear S-Cd-S and Cd-S-S are less stable in comparison to trigonal CdS_2 structure by 0.06 eV. The equilibrium geometry for the triangular CdS_2 structure has a Cd–S bond length of 2.76 Å and S-S bond length of 2.26 Å.

(a) CdS Linear

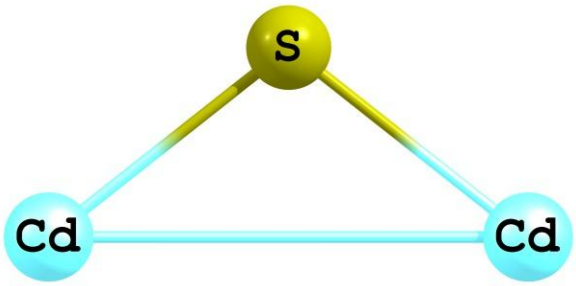

(b) Cd_2S Trigonal

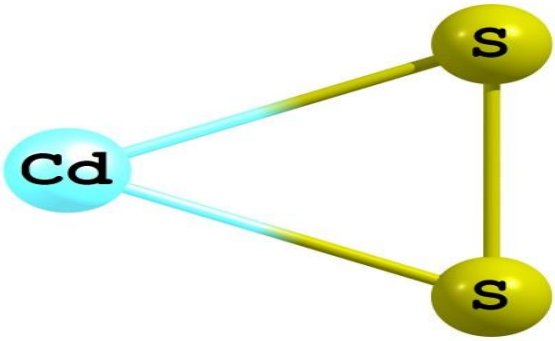

(C) CdS_2 Trigonal

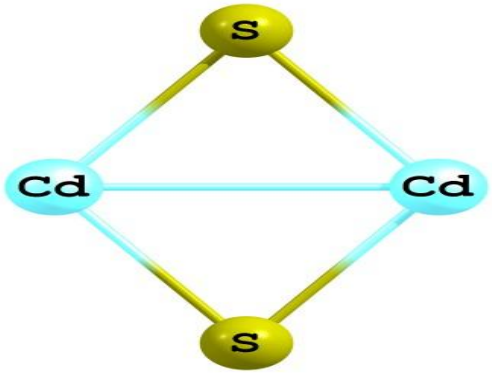

(d) Cd_2S_2 Rhombus

(e) Cd_3S Linear

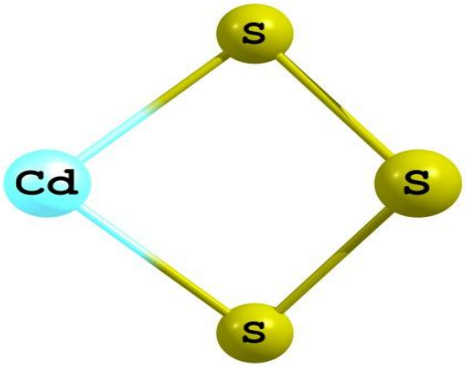

(f) CdS_3 distorted rhombus

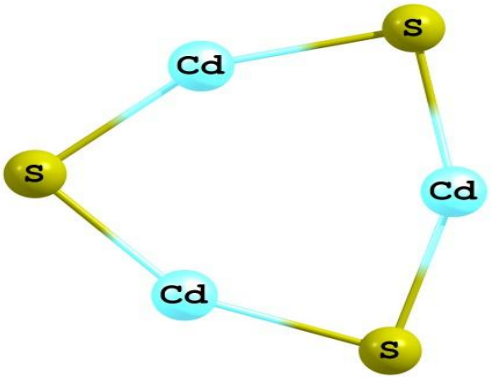

(g) Cd_3S_3 Star

Figure 1: Most stable optimized structures of Cd_mS_n(m+n=2-6) nanoclusters

Table 1. Symmetry, multiplicity of the ground state (GS), binding energy per atom (BE), zero point energy (ZPE), final binding energy (FBE) and HOMO-LUMO gap for all the configuration for the Cd_mS_n(m+n=2-6) Nanocluster

Nanocluster	Configuration	Symmetry	GS Multiplicity	BE (eV)	ZPE (eV)	FBE (eV)	HOMO-LUMO (eV)
CdS	Linear Cd-S	C_{*v}	3	2.39	0.01	2.38	α =4.69 β=3.00
Cd_2S	Linear Cd-S-Cd	C_{*v}	1	1.09	0.03	1.06	α =1.99
	Trigonal	C_S	3	3.08	0.03	3.05	α =3.90 β=2.36
CdS_2	Linear S-Cd-S	D_{*h}	3	2.21	0.05	2.16	α =5.53 β=0.98
	Trigonal	C_S	3	2.26	0.04	2.22	α =3.94 β=1.89
Cd_2S_2	Bent Cd-S-Cd-S	C_1	1	1.63	0.07	1.56	α =0.65
	Linear Cd-S-S-Cd	C_1	1	1.57	0.06	1.51	α =0.90
	Linear S-Cd-Cd-S	C_1	1	1.60	0.05	1.55	α =1.99
	Bent Cd-S-S-Cd	C_1	1	1.57	0.06	1.51	α =1.28
	Rhombus	C_1	1	1.97	0.08	1.88	α =2.23
Cd_3S	Linear Cd-Cd-S-Cd	C_1	1	0.86	0.04	0.82	α =1.73
	Rhombus	C_1	1	0.75	0.0	0.75	α =1.19
CdS_3	Bent S-S-Cd-S	C_1	3	2.23	0.08	2.15	α =4.33 β=2.05
	Rhombus	C_1	1	3.33	0.09	3.24	α =1.82 β=1.82
Cd_3S_3	Hexagon (Caze)	C_1	1	1.55	0.09	1.46	α =2.40
	Hexagon (Star)	C_1	1	2.34	0.14	2.20	α =3.33

Table 2: Symmetry, multiplicity of the ground state (GS), binding energy per atom (BE), zero point energy(ZPE), final binding energy (FBE) and HOMO-LUMO gap for all the most stable configuration for the Cd_mS_n(m+n=2-6) nanoclusters

Nanocluster	Configuration	Symmetry	GS Multiplicity	BE (eV)	ZPE (eV)	FBE (eV)	Other (eV)	HOMO-LUMO (eV)	Other (eV)
CdS	Linear Cd-S	C_{*v}	3	2.39	0.01	2.38		α =4.69 β=3.00	
Cd_2S	Trigonal Cd-S-Cd	C_S	3	3.08	0.03	3.05		α =3.90 β=2.36	
CdS_2	Trigonal S-Cd-S	C_S	3	2.26	0.04	2.22		α =3.94 β=1.89	
Cd_2S_2	Rhombus	C_1	1	1.97	0.08	1.89		α =2.23	2.34[21]
Cd_3S	Linear Cd-Cd-S-Cd	C_1	1	0.86	0.04	0.82		α =1.73	
CdS_3	Rhombus	C_1	1	3.33	0.09	3.24		α =1.82 β=1.82	
Cd_3S_3	Hexagon (Star)	C_1	1	2.34	0.14	2.20		α =3.33	

Table 3: Bond lengths (A°) for all the most stable configurations of Cd_mS_n (m+n=2-6) nanoclusters

Nanocluster	Configuration	Bonds	Bond length (Å) (Present)	(Other)
CdS	Linear Cd-S	Cd-S	2.65	2.295[21], 2.36[35],2.52[36]
Cd_2S	Trigonal	Cd-S	2.59	
	Cd-S-Cd	Cd-Cd	4.06	
CdS_2	Trigonal	Cd-S	2.76	
	S-Cd-S	S-S	2.26	
Cd_2S_2	Rhombus	Cd-S	2.56	2.490[21], ,2.50[35], 2.57[36]
	Cd-S-S-Cd	Cd-Cd	2.96	
		S-S	4.18	
Cd_3S	Linear	Cd-S	2.46	
	Cd-Cd-S-Cd	Cd-Cd	3.24	
CdS_3	Rhombus	Cd-S	2.58	
	S-S-Cd-S	S-S	2.32	
Cd_3S_3	Hexagon	Cd-S	2.49	2.416[21]
	(Star)	Cd-Cd	3.43	

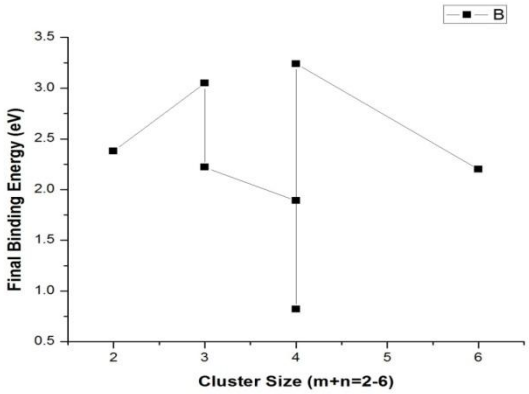

Figure 2: Final binding energy vs cluster size of Cd_mS_n(m+n=2-6) nanoclusters

Cd_mS_n (m+n=4): For the Cd_mS_n (m+n=4) cluster, we have tried for three configurations as Cd_2S_2, Cd_3S and CdS_3 which contain nine geometries structured cluster; and the four atom structured clusters have the singlet ground states. For **Cd_2S_2,** we have investigated five different configurations; two linear structures with Cd-S-S-Cd and S-Cd-Cd-S geometry, two bent structures (Cd-S-Cd-S, Cd-S-S-Cd) and a rhombus structure. From table 1, it is evident that the rhombus structure having C_1 symmetry and ground state of singlet is most stable structure as it has maximum FBE of 1.88 eV. Moreover, results demonstrate that the Cd-S and Cd-Cd bond lengths 2.56Å and 2.96Å respectively are very close to the experimental data (2.57 Å) and the result of Chu et al. [35] (2.50 Å). For **Cd_3S,** three possible structures were tried. These are the two linear chains Cd-Cd-S-Cd and Cd-Cd-Cd-S, and rhombus. From Table 1, it seems logical that the linear (Cd-Cd-S-Cd) geometry with C_1 symmetry has maximum final binding energy of 0.82 eV and is most stable. The computed values of Cd–S and Cd–Cd bond lengths for most stable structure are found to be 2.46Å and 3.24 Å, respectively. For **CdS_3**, we have considered three different geometries; linear chain (Cd-S-S-S), bent (S-S-Cd-S) and rhombus. Among these configurations, most stable structure looks like distorted rhombus with final binding energy 3.24 eV and Cd-S and S-S bond lengths as 2.58Å, 2.32Å, respectively.

Cd_3S_3 (m+n=6): The ground state of six atom nanoclusters is predicted to be singlet. For Cd_3S_3 configuration, we have considered two linear (CdSCdSCdSCdSCdSCdS, CdCdCdSSSS) and two hexagon (Cage, Star) structures. It is found that the most stable structure with highest value of FBE of 2.20 eV, attains hexagon (star) shape having alternate cadmium and sulphur atoms, with three sulphur atoms edge -capping. The calculated Cd- S bond length is 2.49 Å and for the Cd-Cd, bond length is 3.43Å. This value of Cd- S bond length closely approach the data (2.43 Å) deduced by the computations of Chu et al. [35]. The most stable structure has C_1 symmetry and very important one. Thus we see that Cd-Cd bond length is increasing with the size of clusters except the Cd_2S.

3.2. Eectronic Property: HOMO-LUMO and Density of states of CdS nanoclusters

The information about the electronic properties of CdS nanocluster can be known with the help of HOMO-LUMO gap. HOMO–LUMO energy gap depend upon the chemical association and reaction between atoms and molecules.The computed energy gap between the highest occupied molecular orbital (HOMO) and the lowest unoccupied molecular orbital (LUMO) i.e. HOMO–LUMO gap, for all the studied structures is presented in Table

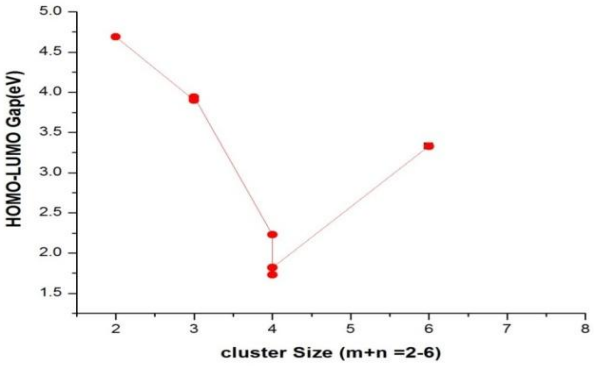

Figure 3: HOMO-LUMO Gap vs cluster size of Cd_mS_n(m+n=2-6) nanoclusters

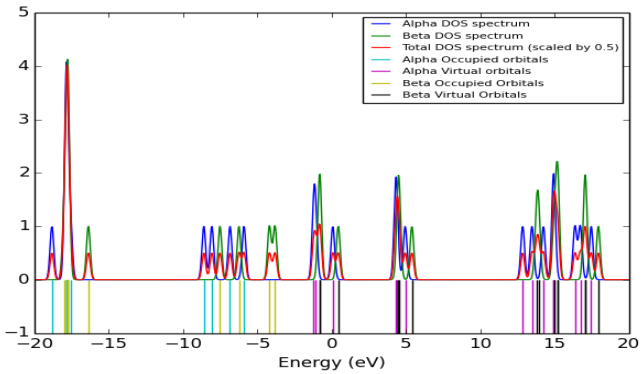

(a) CdS Linear

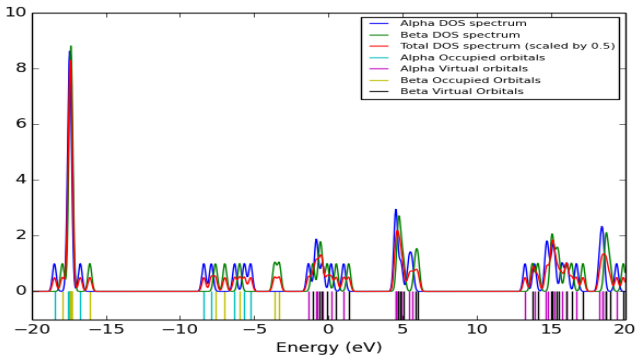

(b) Cd_2S Trigonal

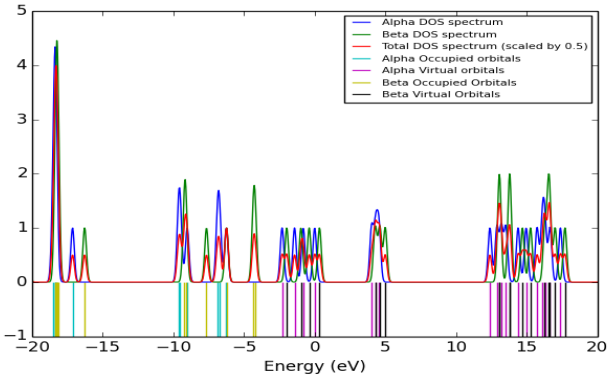

(C) CdS_2 Trigonal

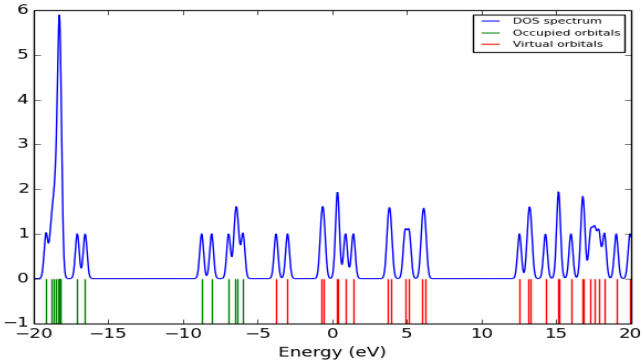

(d) Cd_2S_2 Rhombus

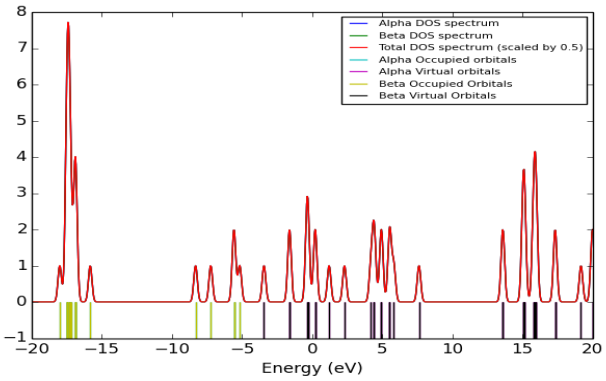

(e) Cd_3S Linear

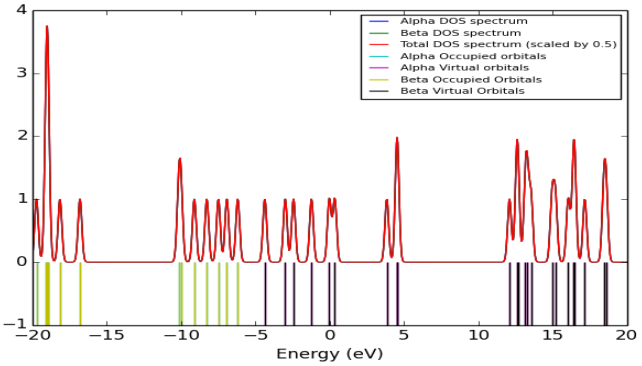

(f) CdS_3 Rhombus

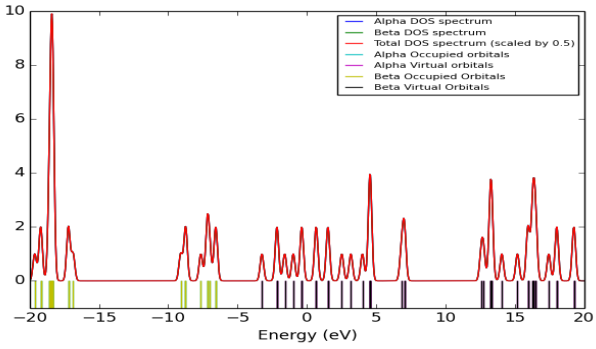

(g) Cd_3S_3 Star

Figure 4: DOS, HOMO_LUMO energy diagram for all the most stable configuration of the Cd_mS_n (m+n=2-6) nanoclusters

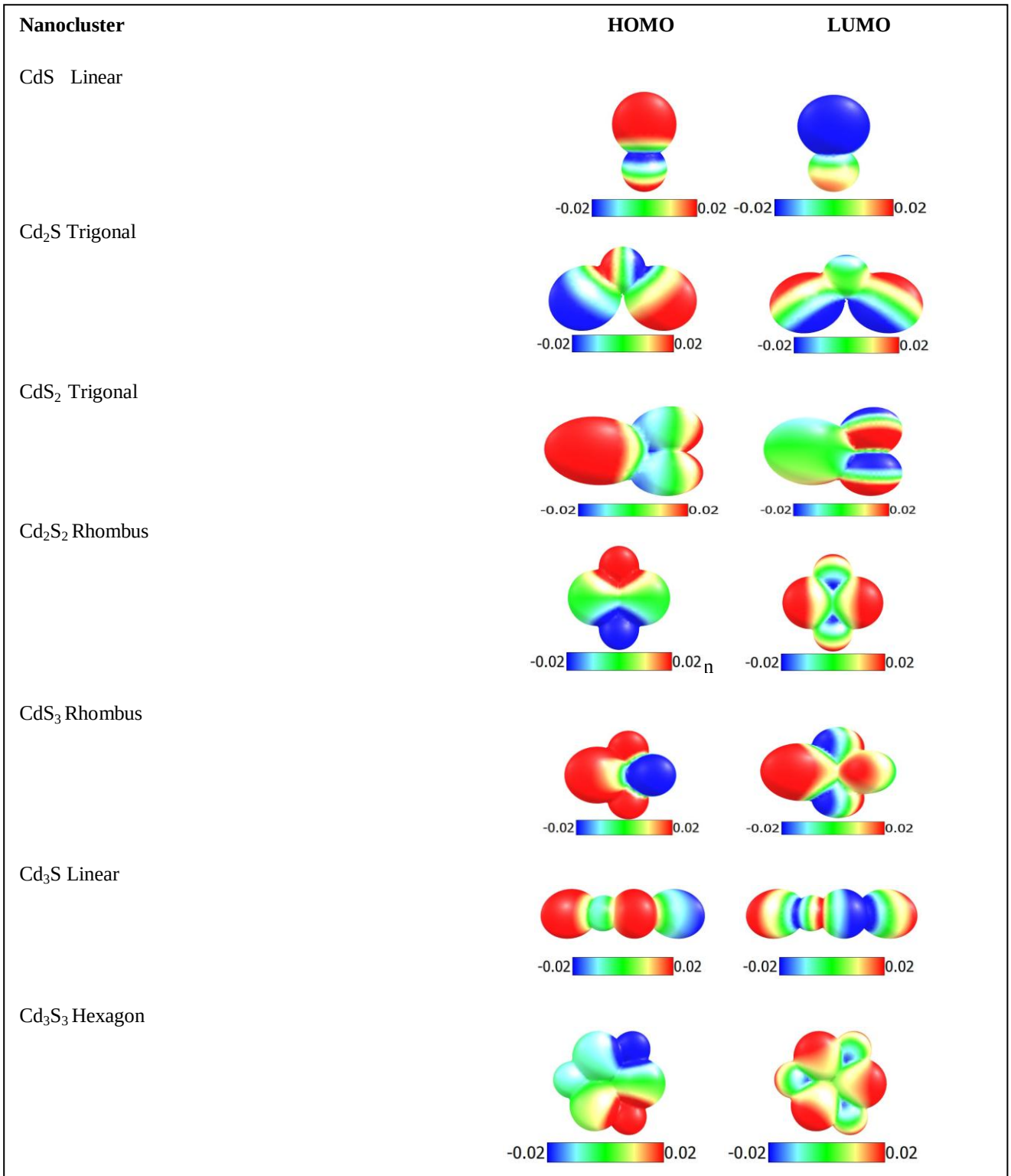

Figure 5: HOMO-LUMO energy visualization for all the most stable configuration of the Cd_mS_n (m+n=2-6) nanoclusters

1. It may be pointed out that HOMO–LUMO gap decrease with number of S atoms; a high energy gap indicates that the cluster is more stable as already noted from the calculated FBEs and also electrons in the valance band needed more energy to go the conduction band. Fig.3 shows the calculated energy gap as a function of cluster size: it is observed that when we increase the size of the nanocluster by adding no. of atoms, HOMO–LUMO gap is rapidly decreasing up to cluster size (m+n)=4 and attains a minimum value of 1.73 eV for Cd_3S configuration. However, it is again rising up to the cluster size (m+n=6) when the cluster size is further increased. As lower energy gap materials are highly reactive in chemical reactions and with catalyst, Cd_3S configuration is highly reactive owing to its lower energy gap. Fig.4 of DOS reveals that due to overlapping of Cd atoms with S atoms in the nanocluster, the density of charge is very low in the occupied orbital than the virtual one. In the cluster, the geometry of the nanoclusters is also affected due to the density of charges in virtual and occupied orbitals. From the Fig.4 it is evident that the DOS is much more depending on the geometry and number of the atoms present in the nanocluster. Further, we observe that for the same and maximum number of m and n i.e. (m+n=4) the amplitude of peak is maximum rather than other clusters. HOMO-LUMO energy visualization for all the most stable configuration of the Cd_mS_n(m+n=2-6) clusters are displayed in fig.5.

3.3. Ionization Potential and Electron Affinity

Ionization potential (IP) and the electron affinity (EA) of a cluster are very important properties from the theoretical point of view. They are experimentally accessible and provide a direct measure for the type of bonding involved in a cluster. The ionization potential (IP) is defined as the amount of energy required to remove an electron from a nanocluster. In the present study, adiabatic ionization potential (AIP) has been calculated by taking the energy difference between the neutral and the ionized nanoclusters after finding the most stable structure for the ionized nanoclusters using the optimization procedure. The electron affinity (EA) is defined as the energy evolved when an electron is added to a neutral cluster. We have evaluated the EA by finding the energy difference between the neutral and the anionic nanocluster; anionic nanocluster is relaxed to its most stable state.

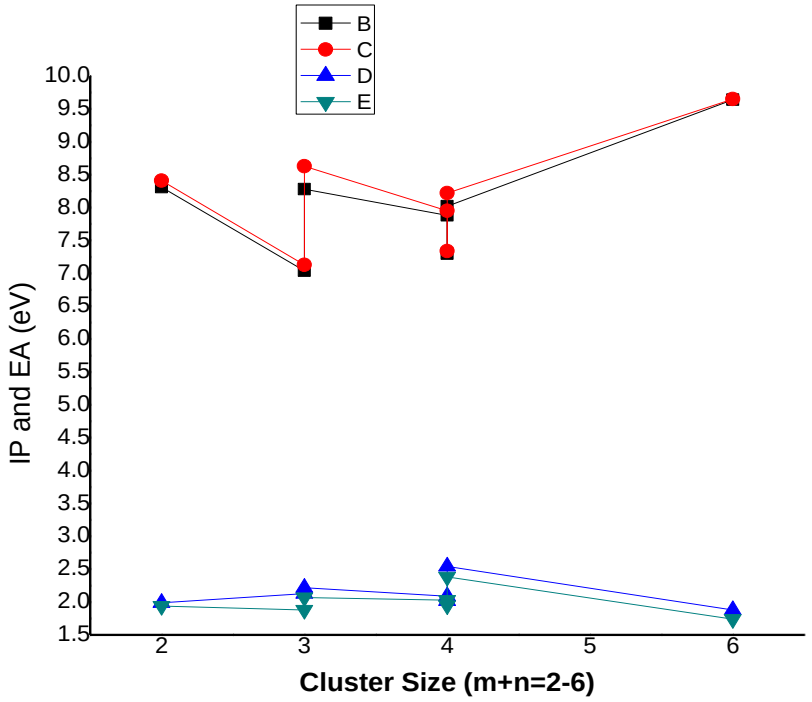

Figure 6: Ionization potential and Electron affinity vs cluster size of Cd_mS_n(m+n) nanoclusters

To the best of our knowledge, experimental data and earlier calculation are available very scarcely for comparison of IP and EA of Cd_mS_n clusters. Adiabatic and vertical IPs and EAs for the most stable structures are listed in Table 4.

Fig. 6 depicts the variation of the adiabatic and vertical IPs and EAs for the most stable structures. A zigzag behavior can be seen in the variation of both IP and EA with nanocluster size. However, similar trend was noted also for the corresponding ZnSe clusters in the literature. It is interesting here to compare the ionization potential. Out of these structures, the hexagon (star (Fig.1g) geometry has the highest value of adiabatic IP and vertical IP, which are 9.64 eV and 9.65 eV; the trigonal structure of the configuration Cd_2S has lowest values of the adiabatic and vertical ionization energy. A perusal of Table 4 shows that the values of the adiabatic and vertical electron affinity for rhombus geometry of CdS_3 configuration are highest i.e. 2.54 eV and 2.38 eV, respectively. For the cluster Cd_2S_2, calculated vertical ionization energy is 7.95 eV which is in good agreement with 8.10 eV evaluated by Sanville et al. [21] and the experimental (7.26 eV) photoelectric thresholds for bulk CdS by Swank [37]. The hexagon (star) structure has the lowest value of adiabatic and vertical EA which are 1.88 and 1.74 respectively.

3.4 . Vibrational Frequencies

Investigation of vibrational frequencies is very significant parameter in exploring the local minimum in the structures. It is observed that even for a small number of atoms in a cluster there are plenty of possible structures which may represent local minima on the energy hyper surface. In order to decide whether or not there is a local minimum, it is necessary to determine the harmonic vibrational frequencies and to check if any of these is zero or takes an imaginary value. In the present investigation, the vibrational frequencies are calculated by the determining the second derivative of the total energy of the system with respect to the atomic displacements at the B3LYP-DFT/LANL2DZ level. The obtained physical quantities for the most stable clusters are listed in table 4. The above physical properties have not been reported by any other worker for the considered nanoclusters. For CdS, we obtain the stretching mode frequency of 209.5 cm^{-1} which is both IR and Raman active. For Cd_2S trigonal (Cd-S-Cd) structure, the calculated frequencies are 41.26 cm^{-1}, 203.25cm-^{1}, 253.08 cm^{-1}. From the table 4, it is evident that highest stretching frequencies are both highly IR and Raman active. The lower frequency 41.26 cm^{-1} originates from the bending vibration of Cd–S bond, etc.

Table 4. The calculated vibrational frequencies (cm^{-1}), infrared intensities (IR Int. in km mol^{-1}), relative IR intensities (Rel. IR Int.) and Raman scattering activities (Raman activity in A^4/amu) for most stable configurations of Cd_mS_n (m+n=2-6) nanoclusters

Nanocluster	Configuration	Properties	Values
CdS	Linear	Frequency	209.53
	Cd-S	IR Int.	2.34
		Rel. IR Int.	1
		Raman activity	49.59
Cd_2S	Trigonal	Frequency	41.26, 203.25, 253.08
	Cd-S-Cd	IR Int.	0.35, 3.38, 24.17
		Rel. IR Int.	0.01, 0.14, 1
		Raman activity	11.52, 52.29, 21.29
CdS_2	Trigonal	Frequency	39.42, 199.18, 449.82
	S-Cd-S	IR Int.	0.02, 23.82, 0.67
		Rel. IR Int.	0.00, 1, 0.03
		Raman activity	33.16, 16.25, 46.37
Cd_2S_2	Rhombus	Frequency	96.86, 128.65, 196.16, 208.96, 309.97, 310.99
	Cd-S-S-Cd	IR Int.	20.10, 0.00, 0.00, 25.14, 44.97, 0.00
		Rel. IR Int.	0.45, 0.00, 0.00, 0.56, 1, 0.00
		Raman activity	0.00, 8.87, 2.64, 0.00, 0.00, 67.69
Cd_3S	Linear	Frequency	6.82, 46.52, 48.22, 50.37, 130.00, 303.36
	Cd-Cd-S-Cd	IR Int.	0.61, 16.33, 2.76, 17.29, 9.74, 79.67
		Rel. IR Int.	0.01, 0.21, 0.03, 0.230.12, 1
		Raman activity	3.10, 2.31, 0.72, 1.12, 18.55, 40.56

CdS_3	Rhombus S-S-Cd-S	Frequency	102.56, 136.69, 240.27, 283.79, 370.78, 379.18
		IR Int.	4.89, 3.17, 3.46, 2.12, 8.58, 10.83
		Rel. IR Int.	0.45, 0.29, 0.32, 0.20, 0.79, 1
		Raman activity	13.12, 30.36, 10.57, 36.62, 6.82, 16.61
Cd_3S_3	Hexagon (Star)	Frequency	59.85, 62.49, 70.37, 70.61, 94.83, 100.67, 262.90, 263.35, 290.11, 293.75, 337.61, 338.35,
		IR Int.	0.01, 0.03, 4.47, 4.51, 27.80, 0.01, 13.42, 13.68, 0.01, 0.01, 72.32, 72.33
		Rel. IR Int.	0.00, 0.00, 0.06, 0.06, 0.38, 0.00, 0.19, 0.19, 0.00, 0.00, 0.99, 1
		Raman activity	0.70, 0.71, 3.18, 3.21, 0.00, 2.74, 11.79, 11.77, 97.73, 0.02, 0.05, 0.04

For CdS_2 trigonal (S-Cd-S) structure, we obtain the frequencies 39.42 cm^{-1}, 199.18 cm^{-1} and 449.82 cm^{-1} wherein the highest frequency of 449.82 cm-^{1} corresponds to the Cd–S stretching vibration. In this case, frequency 199.18 cm^{-1} is found to be highly IR reactive as compared to others. For rhombus Cd_2S_2, (Cd-S-S-Cd) structure, there are six frequencies; the two highest frequencies (310.99 cm^{-1}, 309.97 cm^{-1}) appear due to the breathing of the two S atoms which are not IR active and the remaining four frequencies originate from the mixed vibration of the Cd and S atoms. For Cd_3S, linear configuration has 6 frequencies and the highest frequency of 303.36 cm^{-1} corresponds to the Cd–S stretching vibration which is both IR and Raman active. The rhombus CdS_3 has highest frequency 379.18 cm^{-1} and is found less IR reactive in comparison to the linear Cd_3S configuration.

For Cd_3S_3 hexagonal cage structure, we obtain 12 frequencies in all wherein upper two frequencies 337.61 and 338.35 cm^{-1} are due to the stretching vibration of S atom close to the Cd atom and the lower frequencies 59.85, 62.49, 70.37 and 70.61 cm^{-1} correspond to twisting vibration of whole cluster.

Conclusions

Detailed theoretical characterization of the most stable isomers of the Cd_mS_n(m+n=2-6)nanoclusters have been done using DFT approaches. Bondlengths, adiabatic, vertical ionization potentials and electron affinities and dipole moments for the Cd_mS_n nanoclusters were computed at the same level of theory. The results reveal that the nonlinear structured nanoclusters are most stable in comparison with linear one. We have found that the CdS_3 distorted rhombus structure is most stable among all the considered nanoclusters. Mostly, nanoclusters with high (low) FBEs have large (small) number of sulphur atoms and value of HOMO–LUMO gap deceases with the increase in S atoms. However, the IP and EA both show zigzag behavior with the clusters size. Vibrational properties are studied only for the most stable structures wherein, except the Cd_2S_2 all are IR active at the vibrational frequencies. For the most stable structure CdS_3 the calculated lowest and highest frequencies are 102.56 cm^{-1}, and 379.18 cm^{-1}; both are infrared active. As this approach has produced good results for the CdS, it is possible to extend current study in the modelling and understanding the growth of cadmium-based clusters at the nano scale. This will also motivate new experimental studies on this important class of clusters.

Acknowledgement

The first author is thankful to the UGC, New Delhi, India for the financial support.

References

[1] S.M Woodley, R. Catlow, Nat. Mater, 7937 (2008).
[2] H.J. Himmel, N. Hebben, Chem. Eur. J, 114096(2005).
[3] S.M. Sheehan, G. Meloni, B.F. Parsons, N. Wehres, D.M. Neumark, J. Chem.Phys,124 064303 (2006).
[4] C.B. Murray, D.J. Norris, M.G. Bawendi, J. Am. Chem. Soc., 1158706 (1993).
[5] C. Ricolleaui, L. Audinet, M. Gandais, T. Gacoin, Eur. Phys. J. D, 9565 (1999).
[6] Manna Liberato, C. Erik Scher, L.S. Li, Paul Alivisatos Pau, J. Am. Chem. Soc., 124, 7136 (2002).

[7] B. Song, L. Ling, P.L. Cao, Chin. Phys.,13489(2004).
[8] D. Vogel, P. Kruger, J. Pollmann, Phys. Rev. B, 52 14316 (1995).
[9] A. Tomasulo and M.V. Ramakrishna, J. Chem. Phys. 1053612 (1996).
[10] R. Rossetti, S. Nakahara, L.E. Brus, J. Chem. Phys. 804464 (1983).
[11] R. Rossetti, J.L. Ellison, J.M. Gibson, L.E. Brus, J. Chem. Phys., 791086 (1984).
[12]N. Herron, Y. Wang, M.M. Eddy, G.D.Stucky, D.E. Cox, K. Moller., T. Bein, J. Am. Chem. Soc., 111530 (1989).
[13] P.K. Mahapatra, C.B. Roy, Electrochim. Acta, 291439 (1984).
[14] A.P. Alivisatos, J. Phys. Chem., 10013226 (1996).
[15] M.C. Troparevsky, J. R.Chelikowsky, J.Chem. Phys., 114943 (2001).
[16] P. Deglmann, R. Ahlrichs, K. Tsereteli, J. Chem. Phys., 1161585 (2002).
[17] J. O. Joswig, G. Seifert, T.A. Niehaus, M. Springborg. J. Phys. Chem. B, 1072897 (2003).
[18] J.M. Matxain, J.M. Mercero, J.E. Fowler, J.M. Ugalde, J. Phys. Chem. A, 10810502 (2004).
[19] G.Maroulis, C. Pouchan, J. Phys. Chem. B, 10710683 (2003).
[20] S. Karthikeyan, E. Deepika and P. Murugan, J. Phys. Chem. C, 1165981 (2012).
[21] Sanville, A. Burnin, J.J. BelBruno, J. Phys. Chem. A, 1102378 (2006).
[22] V.S. Gurin, Z. Phys. D, 4265 (1997).
[23] H. Zeng, R.R. Vanga, D.S. Marynick, Schelly, Z.A. J. Phys. Chem. A, 112 14422 (2008).
[24] P. Karamanis, C. Pouchan, Chem. Phys. Lett., 474162 (2009).
[25] J.O. Joswig, M. Springborg. G. Seifert, J. Phys. Chem. B, 1042617 (2000).
[26] J. Frenzel, J. O Joswig, P. Sarkar, G. Seifert, M. Springborg, Eur. J. Inorg. Chem.3585(2005).
[27] J. Frenzel, J. O. Joswig, G. Seifert, J. Phys. Chem. C, 11110761 (2007).
[28] C.E. Junkermeier, J.P. Lewis, G.W. Bryant, Phys. Rev. B, 77205125 (2008).
[29] G.L. Gutsev, O. Neal, R.H. Belay, K.G. Weatherford, C. A. Chem. Phys. 368 113 (2010).
[30] C. He-Ying, L. Zhao-Xia, Q. Guo-Li, K. De-Guo, W. Si-Xin, L. Yun-Cai, D. Zu-Liang, Chin. Phys. B, 17247 (2008).
[31] M.J. Frisch, G.W. Truck's, et-al, Gaussian, Inc., Wallingford CT, 2009.
[32] N. M. O'Boyle, A. L. Tenderholt, K. M Langner, J. Comp. Chem., 29839 (2008).
[33] Chemcraft 1.8, http://www.chemcraftprog.com
[34] Rajkamal Shastri, Deep Kumar, Devesh Kumar, Anil Kumar Yadav, IARJEST, 2 94 (2015).
[35] Chu He-Ying, Liu Zhao-Xia, QiuGuo-Li, Kong De-Guo, Wu Si-Xin, Li Yun-Cai and Du Zu Liang, Chinese Physics B, 172478(2008).
[36] V. S. Gurin, J. Phys. Chem., 100869 (1996).
[37] R. K. Swank, Phys. Rev., 153844 (1967).